From precursor powders to CsPbX3 perovskite nanowires : one-pot synthesis, growth mechanism, and oriented self-assembly

# Precursor Powders-to-$CsPbX_3$ Perovksite Nanowires: One-pot Synthesis, Growth Mechanism and Oriented Self-assemblies

Yu Tong, Bernhard J. Bohn, Eva Bladt, Kun Wang, Peter Müller-Buschbaum, Sara Bals,* Alexander S. Urban,* Lakshminarayana Polavarapu,* and Jochen Feldmann

Dedication ((optional))

**Abstract:** Colloidal synthesis and assembly of semiconductor nanowires continue to attract a great deal of research attention. Here, we demonstrate a single-step ligand-mediated synthesis of single-crystalline $CsPbBr_3$ perovskite NWs directly from precursor powders. Shedding light on the reaction process and morphological evolution reveals that the initially formed $CsPbBr_3$ nanocubes transform into NWs through an oriented attachment mechanism. The optical properties of the NWs can be tuned across the entire visible range by varying the halide (Cl, Br and I) composition through a subsequent halide ion exchange. Single particle studies show that these NWs exhibit strong polarized emission with a polarization anisotropy of 0.36. More importantly, we show that the NWs can self-assemble in a quasi-oriented fashion at an air/liquid interface. This process should also be easily applicable to perovskite nanocrystals of varying morphology for their integration into future nanoscale optoelectronic devices.

Over the past two decades, semiconductor nanowires (NWs) have played an indispensable role in the evolution of nanodevice technologies for a wide range of applications such as sensing, optoelectronics, nanolasers, waveguides, light-emitting diodes and photovoltaics.[1] Despite great progress in the controlled synthesis of high quality semiconductor NWs, full colour tunability has been challenging. However, the rapid emergence of metal halide perovskite nanocrystals (NCs) as a new potential class of semiconductor materials has opened the doors for NWs with wide emission and wavelength tunability through halide composition.[2] Particularly, all inorganic $CsPbX_3$ (X=Cl, Br and I) perovskite NCs have gained special attention owing to their high photoluminescence quantum yields, enhanced stability and the ability to control their morphologies.[3] In spite of the rapid progress made in obtaining shape control of perovskite NCs, with morphologies ranging from nanocubes[3b, 3c] to nanoplatelets[2e, 4] and NWs,[2d, 5] very few attempts have been made toward understanding of the individual growth mechanisms.[2h, 6] Most of the reported synthetic methods generally require inert conditions and a presynthesis of the cesium precursor. However, we have recently shown that precursor powders can be directly transformed into $CsPbX_3$ nanocubes of different halide compositions and nanoplatelets by ultrasonication in the presence of ligand molecules.[3b] In fact, the direct conversion of precursor powders into NCs of a desired morphology can significantly reduce the fabrication time, laborious effort and thus costs of production, all key factors for commercialization. In addition to shape-controlled synthesis, self-assembly of NCs is a crucial step for their integration into devices.[7] Herein, we describe a facile method for the ligand-assisted conversion of precursor powders into single crystalline $CsPbBr_3$ perovskite NWs by ultrasonication (Figure S1). The emission colour of NWs can be tuned across the full visible spectrum by applying a subsequent halide ion ($Cl^-$ or $I^-$) exchange reaction on the $CsPbBr_3$ NWs. Mechanistic studies reveal that NWs are formed through the oriented attachment of the initially formed nanocubes. These NWs show strong polarization-dependent optical properties. Furthermore, we found that these perovskite NWs can self-assemble into quasi-oriented closely packed arrays by an air/liquid interface technique.

The synthesis of colloidal $CsPbBr_3$ perovskite NWs was carried out by adapting the ultrasonication-assisted synthesis of perovskite nanocubes and nanoplatelets developed by our group.[3b] We have found that prolonged ultrasonication under similar reaction conditions leads to the evolution of NWs together with only a few residual nanocubes. A subsequent centrifugation step yields dispersions with NWs of uniform thickness with over 90% purity (Figure S1). The prepared colloidal solution of $CsPbBr_3$ NWs emits pure green emission under UV light illumination as shown in Figure 1a. The corresponding TEM images clearly show the high purity of NWs (width ~12 nm) with a very small percentage of nanocubes (Figures 1c & S1). The as prepared NWs tend to form bundles in the colloidal solution due to strong hydrophobic interactions between ligand molecules, and thus tend to settle down at the bottom of the sample vial due to their larger mass. However, unlike the synthesis of $CsPbX_3$ nanocubes of different halide compositions, $CsPbCl_3$ and $CsPbI_3$ NWs cannot be produced directly.[3b] Instead, the reaction leads to a non-fluorescent yellow phase in the case of $CsPbI_3$ NCs. It is nevertheless possible to tune the emission colour of perovskite NWs across the visible range by applying the well-known halide ion exchange reaction on $CsPbBr_3$ NW templates (Figure 1a).[2f, 8] More importantly, the halide ion

[*] Y. Tong, B. Bohn, Dr. A.S. Urban, Dr. L. Polavarapu, Prof. J. Feldmann
Chair for Photonics and Optoelectronics,
Department of Physics and Center for NanoScience (CeNS)
Ludwig-Maximilians-Universität München,
Amalienstr. 54, 80799 Munich, Germany
E-mail: (urban@lmu.de; l.polavarapu@lmu.de)

Y. Tong, B. Bohn, Dr. A.S. Urban, Dr. L. Polavarapu, Prof. J. Feldmann
Nanosystems Initiative Munich (NIM) Schellingstraße 4 80799 , Munich , Germany

B. Eva, Prof. Dr. S. Bals
EMAT, University of Antwerp,
Groenenborgerlaan 171, B-2020 Antwerp, Belgium
E-mail: sara.bals@uantwerpen.be

K Wang, Prof. Dr. Peter Müller-Buschbaum
Department of Physics, Chair for Functional Materials,
Technische Universität München
James-Franck-Straße 1, 85747 Munich, Germany

Supporting information

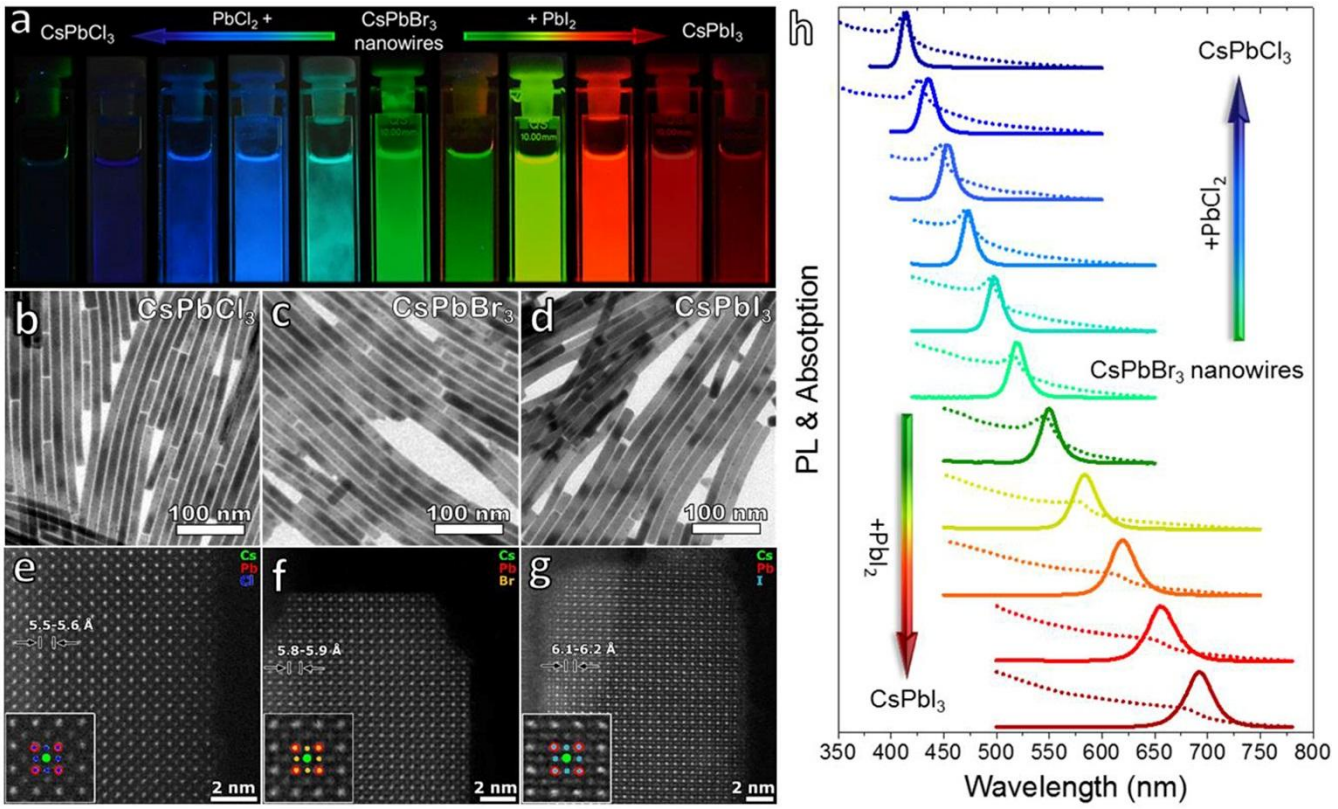


***Figure 1***: (a) Photograph of colloidal dispersions of $CsPbX_3$ perovskite NWs with different halide (X = Cl, Br and I) compositions under UV light illumination ($\lambda$ = 367 nm). $CsPbBr_3$ NWs were obtained by ultrasonication of $Cs_2CO_3$ & $PbBr_2$ in octadecene in the presence of oleylamine and oleic acid. The NWs with mixed halide compositions were obtained by halide ion exchange reactions ($CsPbBr_3$ + $PbCl_2$ (or) $PbI_2$). (b-d & e-g) Bright field-TEM & atomically resolved high resolution HAAD-STEM images of $CsPbCl_3$, $CsPbBr_3$ and $CsPbI_3$ NWs, respectively. (h) Corresponding UV/Vis absorption (dotted lines) and photoluminescence (solid lines) spectra of colloidal $CsPbX_3$ perovskite NWs with different halide (X = Cl, Br and I) compositions.

exchange reaction preserves the $CsPbBr_3$ NW template morphology as evidenced by TEM measurements (Figures 1b & d. See the large area TEM and SEM images in Figure S2) and from high resolution high-angle annular dark field scanning TEM (HAADF-STEM) images recorded along the [100] direction (Figures 1e-g). A difference in the lattice parameters of the NWs is measured, which corresponds to approximately 5.5-5.6, 5.8-5.9 and 6.1-6.2 Å, for $CsPbCl_3$, $CsPBr_3$ and $CsPbI_3$, respectively. X-ray diffraction (XRD) patterns of the NWs (Figure S4) and grazing-incidence wide-angle X-ray scattering (GIWAXS) measurements (Figure S5) reveal that the prepared NWs exhibit either cubic or orthorhombic crystal structures, but they are difficult to distinguish as they exhibit nearly similar diffraction peaks. The crystal structures of the NWs were further studied by high resolution HAADF-STEM and it was found that they exhibit an orthorhombic crystal structure (Figure S3).

The optical properties of the $CsPbBr_3$ NWs before and after the halide ion exchange were characterized by UV/Vis absorption and photoluminescence (PL) spectroscopy. The absorption onset at 524 nm for the Br NWs clearly red-shifts with increasing iodide content and blue-shifts as the chloride content is increased (Figure 1h, dashed lines). Thus, the optical bandgap and PL of the NWs is tunable across the full visible range of 400-700 nm. Additionally, a pronounced excitonic absorption peak can be seen for the Br/Cl NWs indicative of a larger exciton binding energy for these compositions. As depicted in Figure 1h, all colloidal NWs exhibit a single narrow PL emission peak with a small Stokes shift. The emission wavelengths of $CsPbCl_3$ & $CsPbI_3$ NWs are quite similar to the PL emission of nanocubes of the same composition prepared by direct synthesis, thus suggesting the nearly complete replacement of Br with Cl or I.[3b] However, energy dispersive X-ray spectroscopy (EDX) on the NWs indicates that trace amounts of Br are still present after the completion of the halide ion exchange (Figure S6). The shape of the PL emission indicates that the halide ion exchange produces NWs with a single, uniform halide composition rather than NWs comprising different halide ion contents. Time-resolved PL measurements of NWs show that the average PL decay lifetime decreases with decreasing halide ion size (Figure S7), similar to the trend observed for nanocubes in our previous study.[3b] The PL quantum yield (PLQY) of well purified $CsPbX_3$ NWs was found to be significantly lower (0.5%, 10.8%, & 10.3% for Cl, Br & I, respectively) than that of the corresponding nanocubes.[3b] Time-resolved PL measurements further revealed that NWs have a much shorter PL lifetime compared to nanocubes (Figure S8). There are two main possible explanations for the low PLQYs and faster decay of NWs. First, the removal of surface ligands during the purification likely leads to an increase of surface traps and concomitant nonradiative decay resulting from them. The second reason is due to the elongated nature of the wires, which enables a greater exciton delocalization. Through this larger delocalization length, the exciton is far more likely to encounter a trap, leading to nonradiative decay than if the exciton was confined to a single NC. Especially if some of the nanocubes initially contained trap states, greatly reducing their PLQY, then incorporating these into NWs, would greatly enhance the probability that excitons from

neighboring NCs would diffuse to the trap and recombine there via radiative decay. Temperature-dependent PL measurements of $CsPbBr_3$ NWs show that the PL intensity increases strongly with decreasing temperature, in contrast to $CsPbBr_3$ nanocubes, which show nearly no increase (Figure S9). This also suggests that the low PLQY of NWs at room-temperature originates not from a reduced radiative decay, but instead from a higher non-radiative decay, which can be significantly suppressed at lower temperatures. However, the PLQYs of NWs can be improved by excess ligand passivation.[9]

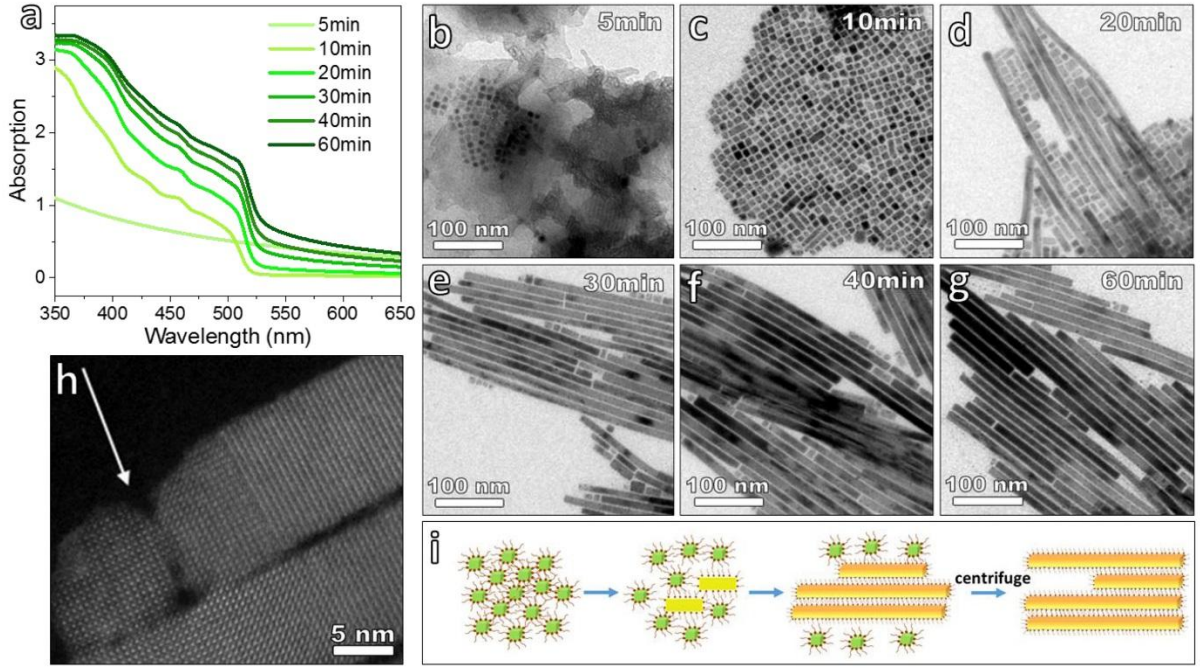


***Figure 2***: (a) UV-Visible extinction spectra of colloidal $CsPbBr_3$ perovskite NCs obtained after different ultrasonication times during the transformation of precursor powders into NWs and their corresponding TEM images (b-g). (h) HAAD-STEM images of $CsPbBr_3$ NCs obtained after 20 min. The arrows show the oriented attachment of nanocubes to NWs. See figure S11 for additional HRSTEM image and corresponding atom-counting results to visualize the oriented attachment (i) Schematic illustration of the transformation of precursor powders into NWs by ultrasonication, in which initially formed $CsPbBr_3$ nanocubes are transformed into NWs.

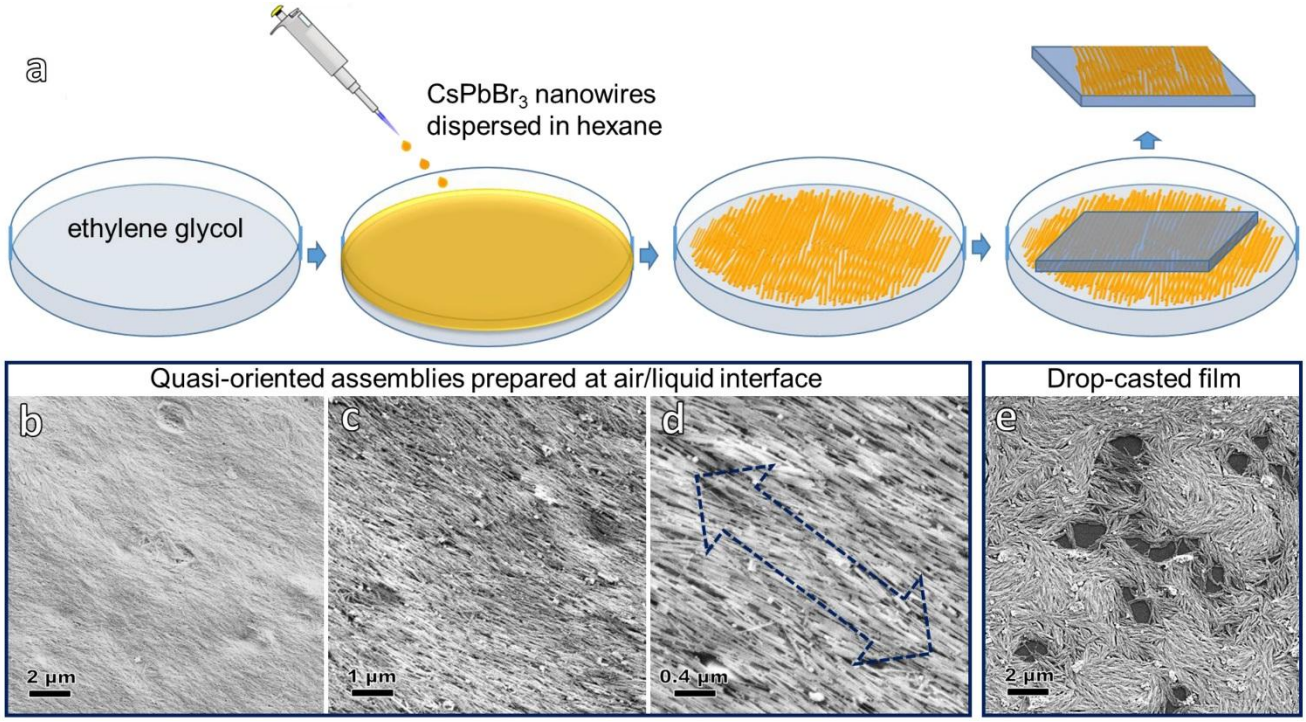


***Figure 4:*** (a) Schematic illustration of the formation of perovskite NW self-assemblies by the air/liquid interface technique. A colloidal perovskite NW dispersion in hexane is dropped onto a ethylene glycol solution in a petri dish. The evaporation of hexane leads to the formation of densely packed quasi-oriented self-assemblies of perovskite NWs at the air/liquid interface. The assemblies are transferrable to any solid substrate applying the Langmuir–Schaefer deposition technique. (b-d) SEM images of quasi-oriented self-assemblies of perovskite NWs prepared at the air/liquid interface. (e) SEM image of a perovskite NW film prepared by a simple drop-casting approach.

In general, inorganic semiconductor NWs are formed either through the oriented attachment of NCs [10] or by surfactant-assisted, seed-mediated anisotropic growth.[11] Both of these growth mechanisms have been proposed for the formation of perovskite NWs, on the basis of TEM analysis.[2d, 3g, 6] To elucidate the formation process of the $CsPbBr_3$ NWs in our synthesis, the reaction was monitored by absorption and PL spectroscopy and complimentary TEM characterization (Figures 2 & S10). The emergence of the steep absorption onset at 520 nm happens quickly, within 10 minutes, and then slightly redshifts over the next 50 minutes (Figure 2a). Additionally, the signal for larger wavelengths increases with synthesis time, indicative of an increased scattering due to larger crystals present in the dispersions. Similarly, the typical single PL peak emerges after 10 minutes. This peak then progressively decreases in intensity with increasing synthesis time, while also slightly red-shifting (see Figure S10 for normalized absorption and PL). TEM analysis of the reaction product at each of these stages shows a significant change in the morphology with synthesis time. At five minutes (Figure 2b) there are only a few small NCs (5-8 nm) visible, with the rest mainly being amorphous structures. After 10 minutes, the reaction product consists of homogeneous nanocubes of 12 nm in size with a small percentage of nanorods, as in our previous report (Figure 2c).[3b] As the synthesis further progresses, NWs begin to appear with lengths on the order of 1-3 µm and lateral dimensions comparable to a single nanocube, while the nanocubes progressively vanish (Figures 2d-f). The percentage of nanocubes significantly decreased after 60 minutes, leaving mainly NWs in the dispersions (Figure 2g). A HAADF-STEM image of NWs obtained after 20 min of reaction clearly showed the oriented attachment of a nanocube to an intermediate nanowire (Figures 2h & S11). Through these optical measurements and the HAADF-STEM analysis we postulate the NWs are obtained through the oriented attachment of nanocubes (Figure 2i). It is worth mentioning that oriented attachment of nanowire formation has been previously reported for silver nanowires.[10] We rule out a seed-mediated growth mechanism, as this process leads to a huge increase in the absorption when a nanocube is transformed into a nanowire,[11] which was not observed in our measurements (Figure S10).

It is has been known that semiconductor NWs generally exhibit anisotropic absorption and PL.[12] We investigated the emission from perovskite NWs in a dark-field microscopy setup (Figure 3a & see the supporting information for more details). The samples were prepared by spin coating a diluted solution of colloidal $CsPbBr_3$ NWs on a cover slide. Individual elongated structures resembling NWs were clearly distinguishable under UV light excitation (inset of Figure 3b). The studied

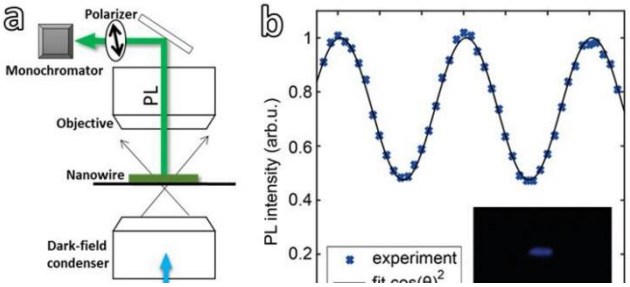


***Figure 3***: (a) Dark field PL image of a $CsPbBr_3$ NW obtained by UV light excitation. (b) Photoluminescence (PL) intensity of $CsPbBr_3$ NWs as a function of emission angle upon excitation with blue light. The PL could be reproduced with a $\cos^2$ function and the polarization anisotropy was found to be ~0.36. The inset in (b) shows the dark field microscope image of a NW bundle under blue light excitation

nanostructures are likely not single NWs, but bundles of parallel oriented NWs, as the observed intensity seems to be too bright for a single NW and due to the fact that the NWs tend to form

aggregates as seen in SEM images. The PL intensity was then acquired as a function of the angle of the polarization filter (Figure 3b). The NWs exhibit a strong polarized emission, which can be well fitted with a cosine-squared function of the polarizer angle (θ). The polarization anisotropy $P = (I_{\parallel} - I_{\perp})/(I_{\parallel} + I_{\perp})$ was calculated to be ~ 0.36 (where $I_{\parallel}$ and $I_{\perp}$ are emission of NWs along the parallel and perpendicular axes of the NW, respectively). This value is comparable to the reported polarization anisotropy of conventional semiconductor NWs such as CdTe NWs and can be attributed to the anisotropic shape of NWs and their parallel alignment.[12]

Besides the synthesis of high-quality colloidal nano-building blocks with excellent control over morphology and composition, their self-assembly into well-defined architectures is essential for device applications. We demonstrate that it is possible to obtain $CsPbBr_3$ NW assemblies at the air/liquid interface.[7] This technique relies on the assembly of hydrophobic nanoparticles by spontaneous evaporation of volatile organic solvents on a hydrophilic liquid surface (Figure 4a), similar to the Langmuir-Blodgett technique.[13] A slight excess amount of oleylamine is added to the colloidal dispersion in order to protect the particles from degradation (see experimental section). The excess oleylamine molecules likely form bilayers on the NW surfaces, preventing the ethylene glycol from reaching the NW surface and degrading it. Furthermore, the hexane, or a similarly volatile organic solvent seems to be necessary, as the NWs degrade, when a less volatile solvent, such as toluene is used instead. The rapid evaporation of the hexane leads to the formation of a NW film floating on the surface of the ethylene glycol, which was then transferred to a silicon substrate for SEM characterization. The NW films obtained at the air/liquid interface consist of densely packed quasi oriented self-assembled NW domains (Figures 4b-d, & S12), in contrast to non-uniform films with randomly oriented NWs obtained through direct drop-casting of the NW dispersions (Figure 4e). The oriented self-assembly process is driven by the minimization of Gibbs free energy of the system through maximum Van der Waals interactions between the ligands on the surface of neighboring NWs. However the self-assembly process failed in the case of $CsPbI_3$ NWs, which were degraded immediately upon coming into contact with the ethylene glycol. Overall, these results suggest that interfacial self-assembled perovskite NCs can be a promising method, but that significant challenges to be addressed in the future remain.

In summary, a single-step ligand-assisted synthesis of precursor powders into single-crystalline colloidal $CsPbBr_3$ NWs of uniform thickness has been demonstrated. The optical bandgap and emission wavelength of the NWs are tunable across the visible light spectrum by varying the halide composition through a subsequent ion exchange reaction. The prepared NWs exhibit strongly polarized emission comparable to some conventional semiconductors. The morphological evolution and corresponding optical properties revealed that the NWs are likely formed through the oriented attachment of nanocubes. Importantly, we have demonstrated the fabrication of quasi-oriented NW self-assemblies at an air/liquid interface, which could be potentially applied to other morphologies. This work not only expands our current understanding of the growth mechanism of perovskite NWs, but is also expected to open new avenues for the fabrication of highly ordered architectures using perovskite NC building blocks for future optical and optoelectronic devices.


**Acknowledgements**

This work was supported by the Bavarian State Ministry of Science, Research, and Arts through the grant “Solar Technologies go Hybrid (SolTech)”, by the China Scholarship Council (Y.T and K.W.), by the Alexander von Humboldt-Stiftung (L.P.), by Flemish Fund for Scientific Research (FWO Vlaanderen) (E.B). S.B. acknowledges the financial support from European Research Council (ERC Starting Grant #335078-COLOURATOMS).

**Keywords:** $CsPbX_3$ perovskite nanowires • ultrasonication • oriented attachment • self-assemblies • polarized emission


**References**


[1] a) N. P. Dasgupta, J. Sun, C. Liu, S. Brittman, S. C. Andrews, J. Lim, H. Gao, R. Yan, P. Yang, *Adv. Mater.* **2014**, *26*, 2137-2184; b) J. Zhang, A. A. Lutich, A. S. Susha, A. L. Rogach, F. Jäckel, J. Feldmann, *Appl. Phys. Lett.* **2010**, *97*, 221915.

[2] a) J. Liu, Y. Xue, Z. Wang, Z.-Q. Xu, C. Zheng, B. Weber, J. Song, Y. Wang, Y. Lu, Y. Zhang, Q. Bao, *ACS Nano* **2016**, *10*, 3536-3542; b) L. C. Schmidt, A. Pertegás, S. González-Carrero, O. Malinkiewicz, S. Agouram, G. Mínguez Espallargas, H. J. Bolink, R. E. Galian, J. Pérez-Prieto, *J. Am. Chem. Soc.* **2014**, *136*, 850-853; c) P. Tyagi, S. M. Arveson, W. A. Tisdale, *J. Phys. Chem. Lett.* **2015**, *6*, 1911-1916; d) D. Zhang, S. W. Eaton, Y. Yu, L. Dou, P. Yang, *J. Am. Chem. Soc.* **2015**, *137*, 9230-9233; e) M. C. Weidman, M. Seitz, S. D. Stranks, W. A. Tisdale, *ACS Nano* **2016**, *10*, 7830-7839; f) Q. A. Akkerman, V. D’Innocenzo, S. Accornero, A. Scarpellini, A. Petrozza, M. Prato, L. Manna, *J. Am. Chem. Soc.* **2015**, *137*, 10276-10281; g) B. Luo, Y.-C. Pu, S. A. Lindley, Y. Yang, L. Lu, Y. Li, X. Li, J. Z. Zhang, *Angew. Chem. Int. Ed.* **2016**, *55*, 8864-8868; h) L. Liu, S. Huang, L. Pan, L.-J. Shi, B. Zou, L. Deng, H. Zhong, *Angew. Chem. Int. Ed.* **2017**, *56*, 1780-1783; i) L. Polavarapu, B. Nickel, J. Feldmann, A. S. Urban, *Adv. Energy Mater.* **2017**, **DOI:** 10.1002/aenm.201700267.

[3] a) S. Sun, D. Yuan, Y. Xu, A. Wang, Z. Deng, *ACS Nano* **2016**, *10*, 3648-3657; b) Y. Tong, E. Bladt, M. F. Aygüler, A. Manzi, K. Z. Milowska, V. A. Hintermayr, P. Docampo, S. Bals, A. S. Urban, L. Polavarapu, J. Feldmann, *Angew. Chem. Int. Ed.* **2016**, *55*, 13887-13892; c) L. Protesescu, S. Yakunin, M. I. Bodnarchuk, F. Krieg, R. Caputo, C. H. Hendon, R. X. Yang, A. Walsh, M. V. Kovalenko, *Nano Lett.* **2015**, *15*, 3692-3696; d) X. Zhang, H. Lin, H. Huang, C. Reckmeier, Y. Zhang, W. C. H. Choy, A. L. Rogach, *Nano Lett.* **2016**, *16*, 1415-1420; e) A. Swarnkar, R. Chulliyil, V. K. Ravi, M. Irfanullah, A. Chowdhury, A. Nag, *Angew. Chem. Int. Ed.* **2015**, *54*, 15424-15428; f) J. Xue, Y. Gu, Q. Shan, Y. Zou, J. Song, L. Xu, Y. Dong, J. Li, H. Zeng, *Angew. Chem. Int. Ed.* **2017**, *56*, 5232-5236; g) M. Chen, Y. Zou, L. Wu, Q. Pan, D. Yang, H. Hu, Y. Tan, Q. Zhong, Y. Xu, H. Liu, B. Sun, Q. Zhang, *Adv. Funct. Mater.* **2017**, *27*, **DOI:** 10.1002/adfm.201701121.

[4] V. A. Hintermayr, A. F. Richter, F. Ehrat, M. Döblinger, W. Vanderlinden, J. A. Sichert, Y. Tong, L. Polavarapu, J. Feldmann, A. S. Urban, *Adv. Mater.* **2016**, *28*, 9478-9485.

[5] D. Zhang, Y. Yang, Y. Bekenstein, Y. Yu, N. A. Gibson, A. B. Wong, S. W. Eaton, N. Kornienko, Q. Kong, M. Lai, A. P. Alivisatos, S. R. Leone, P. Yang, *J. Am. Chem. Soc.* **2016**, *138*, 7236-7239.

[6] T. Udayabhaskararao, M. Kazes, L. Houben, H. Lin, D. Oron, *Chem. Mater.* **2017**, *29*, 1302-1308.

[7] a) A. Sánchez-Iglesias, M. Grzelczak, J. Pérez-Juste, L. M. Liz-Marzán, *Angew. Chem. Int. Ed.* **2010**, *49*, 9985-9989; b) J.-W. Liu, H.-W. Liang, S.-H. Yu, *Chem. Rev.* **2012**, *112*, 4770-4799.

[8] a) G. Nedelcu, L. Protesescu, S. Yakunin, M. I. Bodnarchuk, M. J. Grotevent, M. V. Kovalenko, *Nano Lett.* **2015**, *15*, 5635-5640; b) H. Huang, L. Polavarapu, J. A. Sichert, A. S. Susha, A. S. Urban, A. L. Rogach, *NPG Asia Mater.* **2016**, *8*, e328.

[9] J. De Roo, M. Ibáñez, P. Geiregat, G. Nedelcu, W. Walravens, J. Maes, J. C. Martins, I. Van Driessche, M. V. Kovalenko, Z. Hens, *ACS Nano* **2016**, *10*, 2071-2081.

[10] M. Giersig, I. Pastoriza-Santos, L. M. Liz-Marzan, *J. Mater. Chem.* **2004**, *14*, 607-610.
[11] Y.-N. Wang, W.-T. Wei, C.-W. Yang, M. H. Huang, *Langmuir* **2013**, *29*, 10491-10497.
[12] J. Zhang, A. A. Lutich, J. Rodríguez-Fernández, A. S. Susha, A. L. Rogach, F. Jäckel, J. Feldmann, *Phys. Rev. B* **2010**, *82*, 155301.
[13] A. R. Tao, J. Huang, P. Yang, *Acc. Chem. Res.* **2008**, *41*, 1662-1673.